OPEN ACCESS

University of BRISTOL

Khan, A., Razis, B., Gillespie, S., Percival, C., & Shallcross, D. (2017). Global analysis of carbon disulfide (CS2) using the 3-D chemistry transport model STOCHEM. AIMS Environmental Science, 4(3), 484-501. DOI: 10.3934/environsci.2017.3.484

Publisher's PDF, also known as Version of record

License (if available):
CC BY

Link to published version (if available):
10.3934/environsci.2017.3.484

Link to publication record in Explore Bristol Research
PDF-document

University of Bristol - Explore Bristol Research

General rights

Research article

Global analysis of carbon disulfide (CS_2) using the 3-D chemistry transport model STOCHEM

Anwar Khan[1], Benjamin Razis[1], Simon Gillespie[1], Carl Percival[2,!] and Dudley Shallcross[1,*]

[1] Atmospheric Chemistry Research Group, School of Chemistry, University of Bristol, Cantock's Close, Bristol BS8 1TS, UK
[2] The Centre for Atmospheric Science, The School of Earth, Atmospheric and Environmental Science, The University of Manchester, Simon Building, Brunswick Street, Manchester, M13 9PL, UK
[!] Now at NASA Jet Propulsion Laboratory, 4800 Oak Grove Dr, Pasadena, CA 91109, USA

* Correspondence: Email: d.e.shallcross@bristol.ac.uk; Tel: +44 (0) 117-928-7796.

Abstract: Carbon disulfide (CS_2), a precursor to the long-lived carbonyl sulphide (OCS) is one of the main contributors to the atmospheric sulfate layer. The annual fluxes from its sources and sinks are investigated using a 3-D chemistry transport model, STOCHEM-CRI. In terms of the flux analysis, the oxidation of CS_2 by OH is found to be the main removal process (76–88% of the total loss) and the dry deposition loss contributes 11–24% to the total loss of CS_2. The global burden of CS_2 was calculated, varying between 6.1 to 19.2 Tg and the lifetime of CS_2 was determined to be within the range of 2.8–3.4 days. The global distribution of CS_2 found the Northern Hemisphere (NH) continental landmasses to be the areas of concentration maxima with peak concentrations reaching up to 20 ppt during June-July-August (J-J-A) season and 40 ppt during December-January-February (D-J-F) season in anthropogenic source regions. Oceanic regions returned low CS_2 levels of less than 2 ppt. The vertical profile of CS_2 shows higher levels up to 3 ppt at 30°N–45°N during J-J-A and up to 4 ppt at 30°N–55°N during D-J-F. The oxidation of CS_2 by OH can produce a substantial amount (0.58 Tg/yr) of atmospheric OCS and the annual average surface distribution of this flux shows up to 12 Tg/yr OCS formed in the regions with highest anthropogenic pollution (e.g., South east Asia). In general, the model-measurement comparison reveals an underprediction of model CS_2 compared with measured CS_2 for most of the regions. It is likely that the emissions of CS_2 are being underestimated and there are likely much larger emission sources of atmospheric CS_2 than previously suggested.

Keywords: Carbon disulfide; chemistry transport model; global budget; surface distribution; zonal distribution

1. Introduction

Carbon disulfide (CS_2) exerts a significant influence on the global atmospheric sulfur budget [1,2]. The principal source of CS_2 is supposed to be oceanic [3-8], but spatial analysis of CS_2 indicates large concentrations over continental masses, suggesting the main sources of CS_2 are of anthropogenic origin [9-11]. Blake et al. [11] reported four major industrial sources of CS_2 as black carbon production, rayon manufacture, CS_2 chemical production and use, and sulfur recovery. Ren [12] found that carbonyl sulphide (OCS) converted to CS_2 in the roots and shoots of barley and chickpeas, suggesting it may be a precursor to CS_2 in vegetation and soil. Soil has no consistent flux direction for CS_2 [13]. Soil and wetland fluxes of CS_2 are sparse [10] because of the large variety of soil types (e.g., oxic soils, anoxic soils) and wetland types (e.g., freshwater mangrove swamp, freshwater grassy marsh, and paddy fields) which make them extremely hard to estimate.

The main removal process of CS_2 is the photochemical oxidation with OH radicals producing both sulfur dioxide (SO_2) and OCS as the major products [14,15].

$$CS_2 + OH \rightarrow OCS + SH \tag{1a}$$
$$SH + O(^3P) \rightarrow SO + H \tag{1b}$$
$$SO + O_2 \rightarrow SO_2 + O \tag{1c}$$

The oxidation of CS_2 and the further oxidation of OCS form sulphate aerosols which can influence the radiative properties of the Earth's atmosphere, potentially contributing to climate change and the stratospheric ozone concentration [9,16-20].

CS_2 can also undergo removal by $O(^3P)$ radicals although this is negligible due to low $O(^3P)$ radical abundances in the troposphere [9].

$$CS_2 + O(^3P) \rightarrow CS + SO \tag{2a}$$
$$CS_2 + O(^3P) \rightarrow OCS + S \tag{2b}$$
$$CS + O(^3P) \rightarrow CO + S \tag{2c}$$
$$CS + O_2 \rightarrow OCS + O \tag{2d}$$

The photolysis of CS_2 is possible only in the upper parts of the troposphere by shortwave radiation, but very small at altitudes below 6 km [9].

$$CS_2 + h\nu \rightarrow CS + S \quad (>280 \text{ nm}) \tag{3a}$$
$$CS + O_2 \rightarrow OCS + O \tag{3b}$$
$$S + O_2 \rightarrow SO + O \tag{3c}$$
$$SO + O_2 \rightarrow SO_2 + O \tag{3d}$$

The dry deposition through vegetation can act as a significant loss process of CS_2 [21], but this is not consistent throughout the studies. Taylor et al. [22] reported CS_2 deposition velocities in the range of 0–1.5 mm/s. However, Xu et al. [21] reported CS_2 deposition velocity of 5.6 mm s^{-1} with large associated uncertainties at a spruce forest in the Solling Mountains, Germany. Wet deposition loss is considered to be minimal due to CS_2 being relatively insoluble [23].

The climatic significance of the atmospheric sulfur cycle is difficult to assess without accurate estimation of the global atmospheric reduced sulfur compounds (e.g., OCS, DMS, and CS_2). The

budget for DMS is relatively secure and balanced [10,24,25]; the budget of OCS was previously considered balanced [10,26] but recent studies have shown large uncertainties in its global budget with large missing sources [27-32]. There are very few modeling studies to estimate the global budget and surface distribution of tropospheric CS_2 [3,9,33-35], many uncertainties exist in the assessments of its global budget [10]. In this study, we employ STOCHEM-CRI, a 3-D global chemistry transport model, to evaluate the global budget and distribution of CS_2 in the troposphere. We show a comparison between model CS_2 concentrations and a judicious selection of observed CS_2 concentrations from individual field measurements and some flight data set.

2. Methodology

The global 3-D chemistry transport model, STOCHEM used in this study is from the UK Meteorological Office. This model has been extensively evaluated and assessed in a number of model inter-comparison exercises [36,37], which have shown it to be ideally suited to modeling atmospheric chemistry at a level comparable with Eulerian models. The model uses a Lagrangian approach, where the troposphere is divided into 50,000 air parcels which are advected every three hours by winds from the UK Meteorological Office Hadley Centre general circulation model (GCM). The Lagrangian cells are based on a grid of 1.25° longitude, 0.8333° latitude and 12 unevenly spaced (with respect to altitude) vertical levels with an upper boundary of 100 hPa [38,39]. Each air parcel contains the complete 231 trace gases in the code, which undergo chemical processes. The chemical processes that occur within the parcel, together with emission, dry and wet deposition, mixing and removal processes, are generally uncoupled from advection [39]. During the advection process, the Lagrangian cells are considered to be isolated parcels of air and a treatment of mixing is achieved by imposing a fixed Eulerian grid over the model domain [40]. At each timestep, trace species in Lagrangian air parcels within a Eulerian grid cell are relaxed to the average of the trace species from that group of parcels. Thus, the Eulerian mixing processes are artificially imposed on the Lagrangian parcels to simulate the effects of diffusion in the atmosphere. Turbulent mixing in the boundary layer is achieved by randomly re-assigning the vertical co-ordinates of air parcels over the depth of the planetary boundary layer height. Small-scale convective processes are treated by randomly mixing a fraction of the air parcels between the surface and the cloud top, depending on the convective cloud top, convective cloud cover, and convective precipitation rate. Boundary layer and convection parameterisations were fine-tuned by using ^{222}Rn observations [27]. Other meteorological variables, such as cloud distributions, are kept fixed over the 3-hour chemistry model time-step [41]. More detailed description of the meteorological parameterisations in STOCHEM can be found in Collins et al. [38] with updates described by Derwent et al. [42].

The chemical mechanism used in STOCHEM, is the common representative intermediates mechanism version 2 and reduction 5 (CRI v2-R5). The CRI v2-R5 was developed on a compound-by-compound basis using 5-day box model simulations with the performance of the chemistry for each compound being compared and optimised with the master chemical mechanism (MCM v3.1) with ozone production being the primary criterion. The detail of the CRI v2-R5 mechanism is given by Jenkin et al. [43], Watson et al. [44], and Utembe et al. [45] with updates highlighted in Utembe et al. [39] and Utembe et al. [46]. In the study, the mechanism consists of 231 chemical species competing in 630 reactions and gives excellent agreement with the MCM v3.1 over a full range of NO_x levels [43,44].

Emissions are treated as an additional term to the source fluxes of each species during each integration time step, rather than a step change in species concentration [38,47]. Emission data for

oceans and soil is mapped onto a monthly, 5° longitude × 5° latitude resolution, two-dimensional source map [48]. The anthropogenic surface distribution of CS_2 has been used as like SO_2 surface distribution which were based on EDGAR v3.2 data for 1995 [49]. Total emission values for CO, NO_x, and NMVOCs are obtained from the Precursor of Ozone and their Effects in the Troposphere (POET) inventory [50] for the year 1998 with added emissions of CS_2 from anthropogenic (0.34 Tg/yr), soil + volcano (0.14 Tg/yr) and oceans (0.18 Tg/yr) taken from Watts [10]. Dry deposition is one of the loss processes for CS_2 which is accounted in the model via gravitational movement process. Deposition velocity depends on the location of the air parcel and in the STOCHEM model, there is a distinction made between air parcels over the sea and the land. The dry deposition velocities over land and sea used in the model as 1.5 mm/s [22] and 0.1 mm/s (calculated from the gas transfer velocity based on global average wind speed of ~8 m/s), respectively. The uptake of CS_2 by vegetation with the deposition velocity of 5.4 mm/s [21] was used as dry deposition over land with unchanging deposition over sea (0.1 mm/s) in the model to investigate how the increment of dry deposition over land can affect the global budget of tropospheric CS_2. The photolysis rate of CS_2 in STOCHEM is calculated explicitly for each air parcel at a time resolution of one hour. The photolysis rate of CS_2 is calculated in STOCHEM using the following integral:

$$ J_A = \int_0^\infty F(\lambda)\sigma_A(\lambda)\,\varphi_A(\lambda)d\lambda $$

J_A represents the photolysis rate constant of CS_2;
$F(\lambda)$ represents the spherically integrated actinic flux at a given wavelength;
$\sigma_A(\lambda)$ represents the cross section of CS_2, at a given wavelength;
$\varphi_A(\lambda)$ represents the quantum yield for dissociation of CS_2 at a given wavelength.

The cross-section and quantum yields data were taken from Atkinson et al. [51]. More details about the photolysis reactions implemented in STOCHEM can be found in Khan et al. [52].

The concentrations produced from the model simulation is mapped onto a Eulerian grid resolution 5° × 5° with 9 vertical levels. Summing the 50,000 air parcels produces a global burden for CS_2, which is broken down into the respective source and sink fluxes. The flux outputs are calculated within each grid square by dividing the averaged emissions per air parcel (molecules s^{-1}) by its volume, which gives volume-averaged fluxes with units of molecules cm^{-3} s^{-1}. Five simulations, STOCHEM-base case detailed in Utembe et al. [39], STOCHEM-DEPO with increasing deposition loss of CS_2 over land, STOCHEM-PHOT with including photolysis loss of CS_2, STOCHEM-OCSL with increasing global oceanic and soil emissions of CS_2 and STOCHEM-ANTH with increasing global anthropogenic emissions of CS_2 (Table 1) were conducted with meteorology from 1998 for a period of 24 months with the first 12 allowing the model to spin up. Analysis is performed on the subsequent 12 months of data.

The amount of measurement data from both surface stations and flight campaigns is very limited and thus a judicious selection of data is used to evaluate the model simulations. The simulated data for model-measurement comparison was extracted from the closest grid square to the region in question. Some experimental data was taken for a large area and thus encompasses many grid boxes and in such circumstances, data were extracted from multiple grid squares and the average was taken. The modeled data are monthly averages for a given region adjusted to represent the months studied.

Table 1. Details of the simulations performed in the study.

Model simulation	Loss processes	Deposition velocity (mm/s)	Emission class
STOCHEM-base	$CS_2 + OH \rightarrow$ Products $k_1 = 1.25 \times 10^{-16}\exp(4550/T)/(1 + 1.81 \times 10^{-13}\exp(3400/T))$ cm^3 molecules^{-1} s^{-1} [53] $CS_2 + O(^3P) \rightarrow$ Products $k_2 = 3.2 \times 10^{-11}\exp(-650/T)$ cm^3 molecules^{-1} s^{-1} [53]	Land-1.5 Ocean-0.1	Anthropogenic-0.39 Tg/yr, soil-0.09 Tg/yr, ocean-0.18 Tg/yr [10]
STOCHEM-DEPO	Same as base case	Land-5.4 [21], Ocean-0.1	Same as base case
STOCHEM-PHOT	Same as base case and an additional reaction, $CS_2 + h\nu \rightarrow$ Products	Same as STOCHEM-DEPO	Same as base case
STOCHEM-OCSL	Same as STOCHEM-PHOT	Same as STOCHEM-DEPO	Anthropogenic-0.39 Tg/yr, soil-0.9 Tg/yr, ocean-0.7 Tg/yr [3]
STOCHEM-ANTH	Same as STOCHEM-PHOT	Same as STOCHEM-DEPO	Anthropogenic-1.77 Tg/yr, soil-0.17 Tg/yr, ocean-0.58 Tg/yr [54]

3. Results and Discussion

3.1. Global budget of CS_2

Table 2 details the production and loss processes of CS_2. In this study, only the direct emissions of CS_2 from anthropogenic sources, oceans, soils had been integrated into the model. Three sinks of CS_2 were identified in the STOCHEM-base case: the reaction with OH, the reaction with $O(^3P)$ and the dry deposition. Oxidation by OH radicals is found to be the main sink of CS_2 (0.58 Tg/yr, 88% of the total sinks), which is concordant with the data estimates (0.57 Tg/yr) from Chin and Davis [9] and Watts [10] who estimated that oxidation by OH accounts for 56–100% of CS_2 removal. The simulated flux of the CS_2 conversion to OCS contributes 43% of the total production flux of OCS (1.31 Tg/yr) estimated by Watts [10]. The concentrations of $O(^3P)$ are very low across the troposphere and hence the contribution of the loss process, $CS_2 + O(^3P)$ is found to be very small (<1%) in the study. The dry deposition is another sink of CS_2 (0.07 Tg/yr, 11% of the total loss) which has been found to be significant (0.15 Tg/yr, 23% to the total loss) after a 5-fold increment of deposition velocity over land in the simulation, STOCHEM-DEPO. The emission fluxes of CS_2 from the previous four modeling studies [3,33-35] with a range of global emissions (0.4–2.4 Tg/yr) of CS_2 used in their models (Table 2) gave a range of global burdens (7.8–80 Gg) and lifetimes (4–13 days). However, in our model study, the global burden of CS_2 is found to be small compared with the studies of Pham et al. [33], Weisenstein et al. [34] and Khalil and Rasmussen [3], the discrepancy in emission data is the likely reason for the disagreement between the results. The simulated lifetime of CS_2 for the STOCHEM-base is found to be 3.4 days, which is at the lower end of the range of literature estimates shown in Table 2. The photolysis of CS_2 has been ignored in all previous modeling studies [35], but we included the photolysis of CS_2 in STOCHEM-PHOT and found this

loss process very negligible (0.01 Gg/yr) compared with other loss processes. The inclusion of emission classes of Khalil and Rasmussen [3] in STOCHEM-OCSL (increased global soil and oceanic emissions in the model) and Lee and Brimblecombe [54] in STOCHEM-ANTH (increased global anthropogenic emissions in the model) increases the global burden of CS_2 to 16.2 Gg and 19.2 Gg, respectively which are 212 and 271% increments relative to the STOCHEM-PHOT. Thus, when emissions are the only atmospheric source of a compound, a range of emission classes makes it difficult to ensure an accurate and valid output from a modeling study. The oxidation of CS_2 by OH in STOCHEM-OCSL and STOCHEM-ANTH can provide a substantial amount of atmospheric OCS, 1.6 Tg/yr and 1.9 Tg/yr, respectively.

Table 2. The global budget of CS_2. The values (except global burden and lifetime) given are masses of CS_2 in Tg/yr for the total production and loss. The percentage contributions of the loss processes are shown in parenthesis.

|	STOCHEM-base	STOCHEM-DEPO	STOCHEM-PHOT	STOCHEM-OCSL	STOCHEM-ANTH	Pham et al. [33]	Kjellström [35]	Weisenstein et al. [34]	Khalil and Rasmussen [3]
Production									
Direct emission	0.66	0.66	0.66	1.99	2.52	1.19	0.43	2.38	2.0
Removal									
OH oxidation	0.578 (88.4)	0.504 (77.0)	0.504 (77.0)	1.583 (80.5)	1.890 (75.7)	1.19	0.43	2.35	0.6
Reaction with $O(^3P)$	0.002 (0.3)	0.001 (0.2)	0.001 (0.2)	0.004 (0.2)	0.005 (0.2)	n/a	n/a	n/a	n/a
Dry deposition	0.074 (11.3)	0.149 (22.8)	0.149 (22.8)	0.379 (19.3)	0.602 (24.1)	n/a	n/a	n/a	0.1
Photolysis	n/a	n/a	0.00001 (0.0)	0.00001 (0.0)	0.00004 (0.0)	n/a	n/a	n/a	0
Other									1.3
Global Burden (Gg)	6.11	5.18	5.19	16.17	19.23	11.8	7.8	45.1	70.0
Lifetime (days)	3.4	2.9	3.0	3.0	2.8	4.0	6.5	7.0	13.0

Notes: *n/a represents no available data.

3.2. Global surface distribution of CS_2

The surface distributions of CS_2 in STOCHEM-base (Figure 1) show a difference between the continental regions in the northern hemisphere (NH) and southern hemisphere (SH) with increased CS_2 concentrations of up to 20 pptv during June-July-August (J-J-A) and up to 40 pptv during December-January-February (D-J-F) over anthropogenic emission regions (e.g., North America, central Europe and South East Asia) in the NH. The surface distribution pattern of CS_2 in our model is comparable with the studies of Pham et al. [33] and Kjellström et al. [35] who also found highest concentrations of CS_2 over areas of industrial activity. However, the magnitude of surface CS_2 levels in our study is found to be more variable than their studies which are most likely due to the different emission classes used in the models as well as because of the different resolutions of the models. For example, the emissions total used in STOCHEM (this study) is slightly higher than that used in

IMAGES by Pham et al. [33], but 2-fold lower than that used in ECHAM3 by Kjellström et al. [35] (see Table 2), but the vertical resolution of STOCHEM (9 vertical levels) is coarser than that of IMAGES (25 vertical levels) and ECHAM3 (19 vertical levels). The surface layer is taken between the surface and 1 km in STOCHEM compared with the models IMAGES and ECHAM3 which were taken from 30–35 m and therefore much greater dilution by mixing and removal that can take place in STOCHEM. Thus, the decreased vertical resolution of STOCHEM may give rise to the lower mixing ratios of CS_2 from areas of increased anthropogenic emissions.

The east coast of the US and South East Asia reach elevated concentrations of up to 20 pptv during J-J-A (Figure 1A) which reflects the increased industrial activities of these areas. Europe has background CS_2 concentrations of between 3–7 ppt with several hot spots of high CS_2 concentrations reaching up to 15 ppt over Eurasia (e.g., Turkey) and the Middle East (e.g., Iraq, Saudi Arabia) (Figure 1A) most likely attributed to the oil, gas, and petrochemical industries as well as increased anthropogenic pollution. There are a few hot spots of CS_2 (e.g., 10 ppt) in the southern continental regions such as South Africa (Figure 1A). The elevated CS_2 concentrations around South Africa are expected because of its significant petrochemical, plastic, and synthetic fibre industries [55]. In South America, there appear to be two areas (e.g., near Rio de Janeiro and Northern Brazil) of increased CS_2 concentrations (2–3 ppt) are most likely to be due to increased anthropogenic emissions partly due to the high population densities in these places.
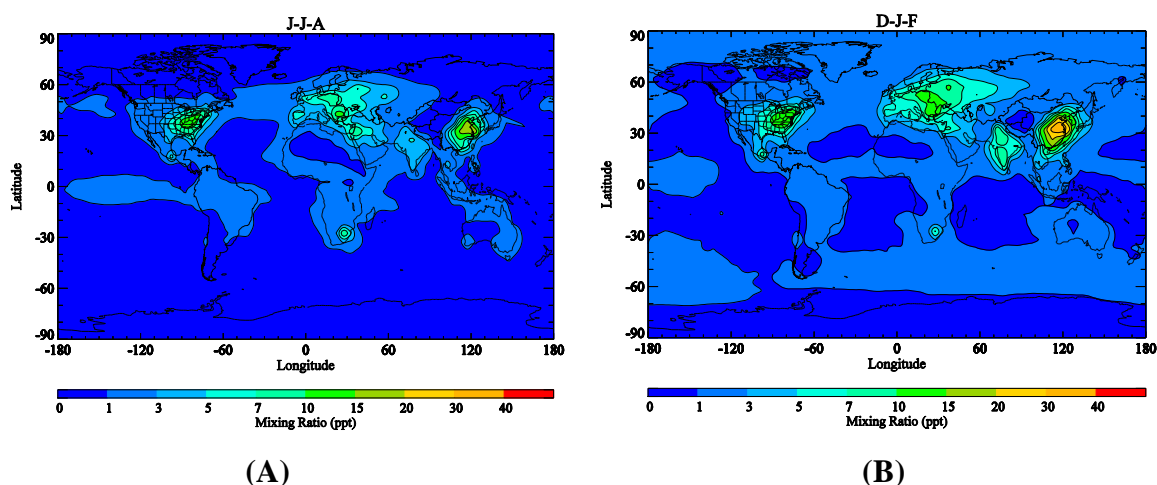

Figure 1. The average surface level distribution of CS_2 simulated by the STOCHEM-base for (A) J-J-A and (B) D-J-F seasons.

During D-J-F, there is a significant increment in concentrations over the continental landmasses (e.g., up to 40 ppt in south East Asia, Figure 1B). This is to be expected as removal by OH accounts for 88% of CS_2 removal and in D-J-F months, OH concentrations in the NH are far lower than that of the J-J-A months. The global oceanic emissions of CS_2 (0.18 Tg/yr) integrated in the STOCHEM-base model resulted in the concentrations of CS_2 between 1 to 3 ppt in most of the oceanic regions. This indicates that 3 ppt is the annual average upper limit of CS_2 concentrations from open ocean. In a variety of open ocean areas regions exist with concentrations of less than 1 ppt.

The inclusions of increased soil and oceanic emissions in STOCHEM-OCSL and increased anthropogenic emissions in STOCHEM-ANTH increase the concentration of CS_2 relative to the

STOCHEM-PHOT by up to 800% (Figure 2A) in the regions of Amazon rainforest, central and southern Africa and Australia and by up to 400% in the regions of North America, central Europe and South East Asia (Figure 2B), respectively. These increased amounts of CS_2 can enhance the oxidation products (e.g., OCS, SO_2) which can alter the formation of the global atmospheric sulfate layer.
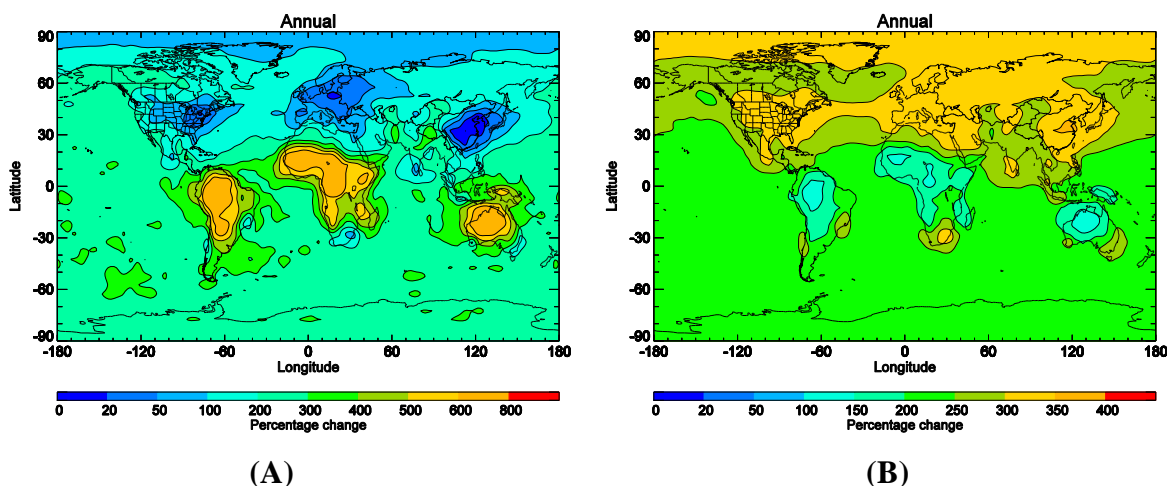

Figure 2. The percentage change of surface CS_2 level (A) from STOCHEM-PHOT to STOCHEM-OCSL and (B) from STOCHEM-PHOT to STOCHEM-ANTH.

CS_2 is the most important precursor gas to OCS, for which a large missing source is needed to balance sources and sinks [28-32]. The flux analysis using the STOCHEM-base model shows that up to 12 Tg OCS /yr per grid box can be formed from the reaction CS_2 + OH in the regions (Figure 3A) with very high anthropogenic pollution (e.g., South east Asia). Incorporating the global anthropogenic emissions of CS_2 [54] in the STOCHEM-ANTH model produces up to 40 Tg OCS /yr per grid box in South East Asia (Figure 3B). This revised production of OCS from CS_2 can play an especially important role over South East Asia regions, where comparisons between measurements and anthropogenic emission inventories show a significant missing source of OCS [11].
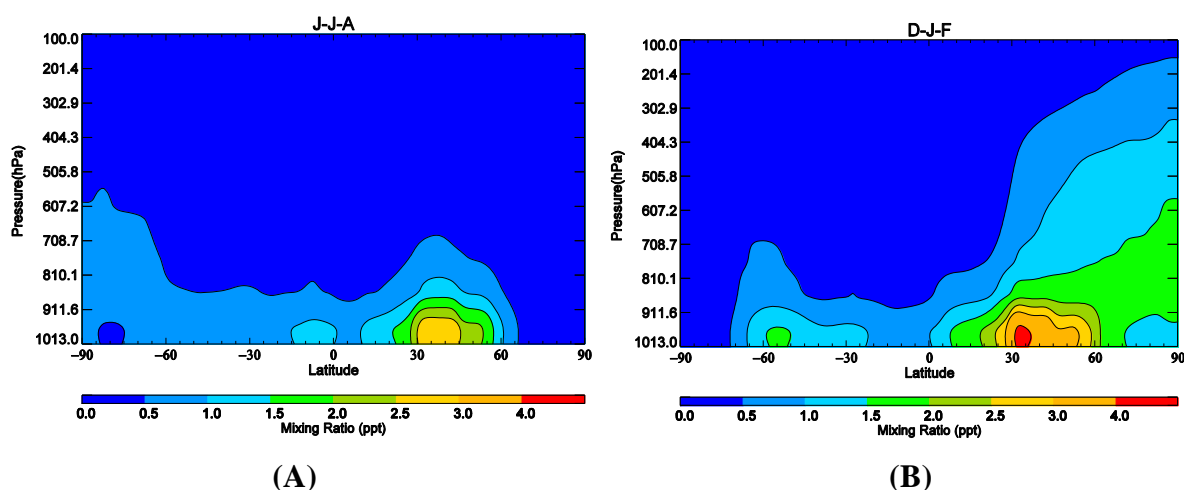
3.3. Global vertical distribution of CS_2

The vertical profile data in STOCHEM-base (Figure 4) shows the decay of CS_2 concentrations as altitude increases. The J-J-A season vertical distribution shows higher levels of CS_2 up to 3 ppt at 30°N–45°N (Figure 4A) due to the larger surface concentrations over the latitude due to areas of high anthropogenic emissions from Europe and North America. A very small area (0–15°S) of higher CS_2 (1.5 ppt) is visible in the tropics (Figure 4A) because of the increased oceanic emissions. Heading south from 30°S latitude to 90°S, CS_2 is found in small amounts throughout the troposphere. In general, the model OH concentration decreases from the equator for each altitude bin, and so the loss of CS_2 via reaction with OH decreases in a similar way (Figure 4A). During D-J-F, the CS_2 concentration is also found to be higher (up to 4 ppt) in the region of 30–55°N (Figure 4B) due to the larger anthropogenic activity, but the vertical distribution of CS_2 for D-J-F mirrors that of J-J-A; lower OH concentration in the NH during D-J-F leads to lower removal of CS_2 and therefore it can reach higher altitudes in the region of 60–90°N. During D-J-F, the peak in the tropics disappears due

to the decreased emissions from ocean but another peak at the region of 50–60°S appears due to the increased emissions from SH oceans.
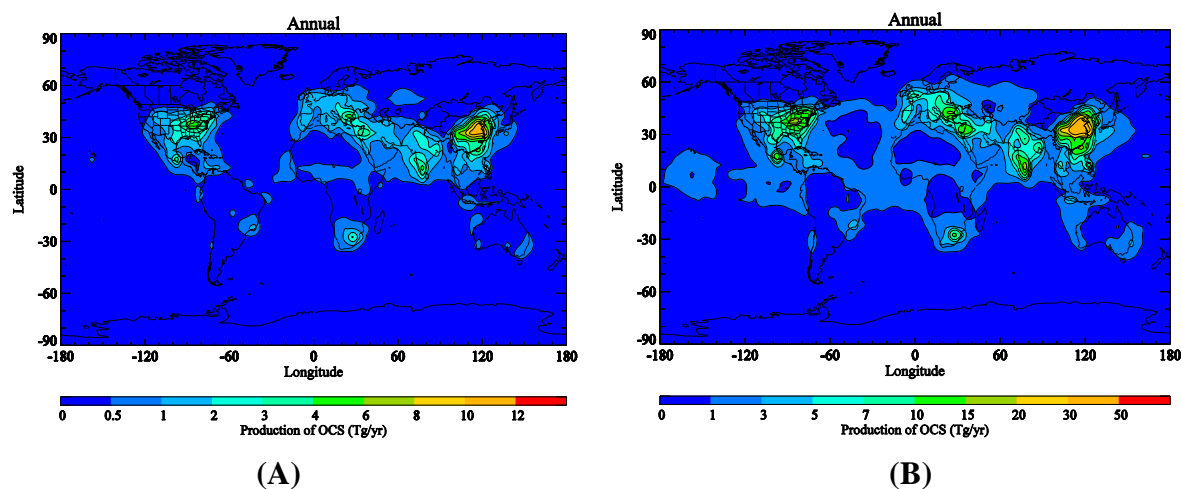
Figure 3. The annual average surface distribution of OCS production from the oxidation of CS$_2$ simulated by (A) the STOCHEM-base (B) the STOCHEM-ANTH.

Figure 4. The average zonal distribution of CS$_2$ simulated by the STOCHEM-base for (A) J-J-A and (B) D-J-F seasons.

The vertical CS$_2$ distribution shows similarities to the vertical profile found by Kjellström [35]. Both profiles display peaks around 60°N and 60°S, but the concentrations seen in this study are found to be smaller than that in Kjellström [35]. Ultimately, as the emission data and the resolution of the two studies are different, it is unsurprising that the absolute concentrations are different, yet what is encouraging is that despite these factors, the annual vertical distributions are similar.

3.4. Model-measurement comparison

In order to develop an understanding of the model accuracy, data points were extracted from the model and compared with 12 field measurements and 9 flight data sets (Table 3). The model uses meteorological data from 1998, but the field and flight data sets were taken from different studies for 1979–2005 which were combined in the same plot panels in Figures 5 and 6, this could involve potential artefactual patterns from using different measurement methods/sampling times. The simulated CS_2 data shows no clearly defined seasonal cycle (Figure 5). The seasonal cycle of CS_2 is controlled by seasonality in their emissions, losses (by OH, deposition) and atmospheric transport. The loss process due to higher OH concentrations during summer would produce the seasonal cycle of summer minimum with winter maximum. However, the oceanic emissions would be highest in summer months and lowest in winter months. Little is known about the production mechanisms of CS_2 in the ocean (one of the major sources of CS_2), but evidence suggests that the production can be through photochemical and biological processes [6,7]. The competition between oceanic emissions and loss by OH resulted in a complex seasonal cycle of CS_2 which is reflected in Figure 5.

Table 3. Details of the respective locations and time period analysed in the model study.

Locations	Longitude-Latitude	Time	Reference
Gosan, Jeju Island, Korea	33°N, 127°E	April 2001	[56]
Tai O, Hong Kong	22°N, 114°E	March–May 2002	[57]
Ansan, South Korea	37°N, 127°E	Aug 2004–Sep 2005	[58]
Beijing, China	40°N, 116°E	Nov 2001	[59]
Philadelphia, PA, USA	40°N, 75°W	Nov–Dec 1979	[60]
Wallops Island, VA, USA	37°N, 75°W	Dec 1979	[60]
Harwell, UK	52°N, 1°W	Jan 1981	[61]
Nadi, Fiji	17°S, 177°E	Feb 1987	[62]
Fremantle, Australia	32°S, 116°E	Nov–Dec 1996	[63]
North Atlantic (Coastal)	27–40°N, 72–80°W	Apr–Sep 1986	[5]
North western Pacific, eastern Indian and Southern Ocean	40°N–60°S, 110–140°E	Nov–Dec 1996	[63]
Southern Ocean	60–66°S, 40–110°E	Nov–Dec 1996	[63]
North Atlantic	32–40°N, 70–75°W	Aug–Sep 1989	[64]
South Tropical Atlantic	2°N–12°S, 25–35°W	Aug–Sep 1989	[64]
Japan sea coast	35–36°N, 135–136°E	Dec 1995, Apr 1996	[65]
Western Pacific	10–35°N, 115–165°E	Feb–Apr 2001	[11]
Central/Eastern Pacific	10–35°N, 165–230°E	Feb–Apr 2001	[11]
Wallops Island, Virginia to Natal, Brazil	39°N–6°S, 35–75°E	Sep 1989	[66]
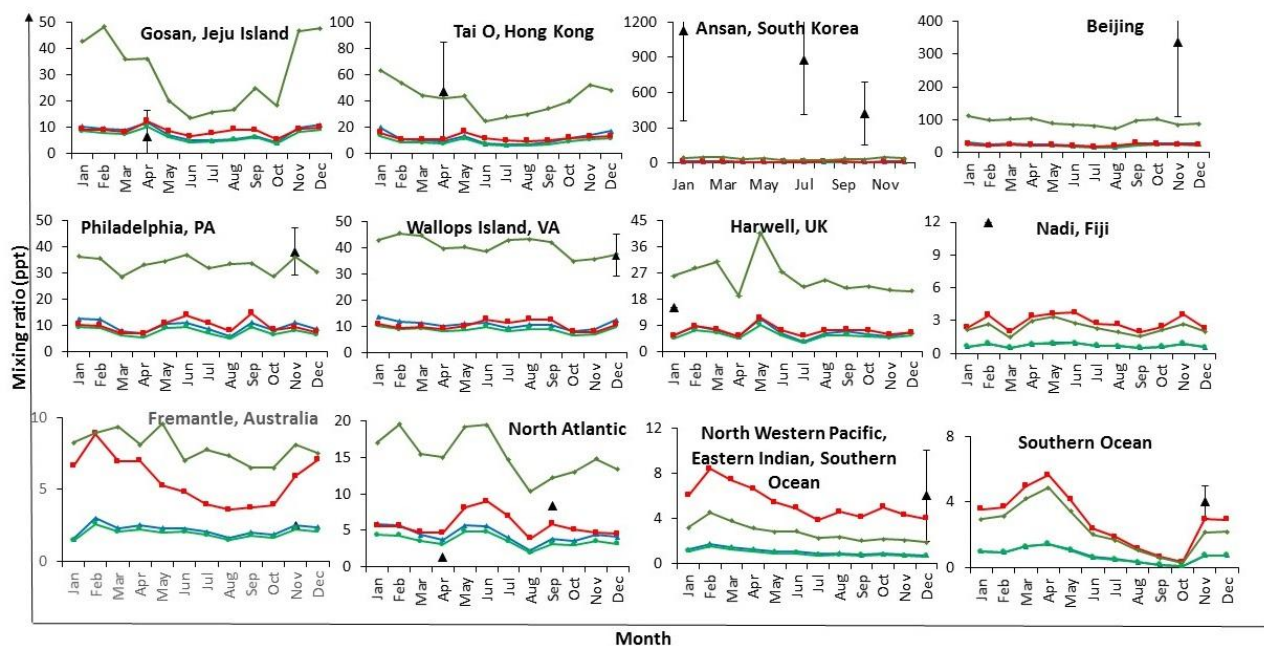
Figure 5. Monthly variation of the surface CS₂ abundances of selected monitoring stations produced by the STOCHEM-CRI. Blue, green, red and bottle green lines represent mean calculated values of CS₂ produced by the STOCHEM-base, the STOCHEM-DEPO, the STOCHEM-OCSL, and the STOCHEM-ANTH, respectively. Black triangle symbols represent the measurement data of CS₂ and the error bars represent measurement variability.

The area best modeled is the marine boundary layer likely due to this area being subject to insignificant amounts of anthropogenic emissions, but an underprediction with a mean bias of −2.7 ppt for the modeled data compared with the measured data is found when looking at regions within marine clean environments (e.g., North Atlantic, Southern Ocean, Pacific, eastern Indian and Southern Ocean). The global oceanic emissions of CS₂ are highly variable ranging from 3.3 to 2346 Gg/yr for different marine environments [8], but we used the global oceanic emissions of 180 Gg/yr in the STOCHEM-base case which can explain the discrepancies between model and measured CS₂ in the marine environment. Increasing the global soil and oceanic emissions [3] in the STOCHEM-OCSL brings the model into closer agreement (mean bias reduces to −0.6 ppt) with measurements for these marine campaigns. The oceanic emissions of CS₂ are unclear because of lacking process understanding, a further investigation into how the discrepancies can be improved would be highly desirable.

The correlation between modeled and measured CS₂ is found to be very good for some clean areas (e.g., Jeju Island in Korea, Fremantle in Australia), but the CS₂ concentrations in approximately background air (relatively unpolluted air) arriving at the east coast of the USA, Philadelphia and Wallops Island and in air arriving at rural areas Harwell, UK and Tai O, Hong Kong are reported as 36 pptv in November, 40 pptv in December, 15 pptv in January and 47 pptv in March-April-May, respectively [56,59,60] which equates to a large underprediction (mean bias of −24.7 ppt) of the simulated values by STOCHEM-base (Figure 6). Harwell and Tai O are located in the rural environment, but there are nearby industrialized areas which may contain large anthropogenic sources of CS₂ which can be advected into the rural areas increasing the ambient rural conditions.

Increasing the global anthropogenic emissions of CS_2 in the STOCHEM-ANTH model improves the agreement with measurements (the mean bias reduces to -1.0 ppt) for these locations. Relatively low concentrations of simulated CS_2 are found in Fiji which are likely to be due to the absence of significant anthropogenic sources surrounding the area. The measured data collected near Fiji recorded concentrations as high as 12 pptv, because there are significant biomass burning events in the area [62], which may have skewed the results and therefore may be unrepresentative of Fiji's natural ambient condition. Due to limited data within the remote SH and hence clean atmospheric conditions, this hypothesis couldn't be tested any further. Increased experimental data within the remote SH would help to validate global atmospheric models and perhaps filling this void should be a focus of future expeditions.

Air samples collected from industrial areas (e.g., Beijing, China and Ansan, South Korea) found very high concentrations of CS_2 due to the anthropogenic emissions, giving very large underprediction of the STOCHEM-ANTH modeled values with a mean bias of -490 ppt compared with the measured values. Due to the large difference in magnitude it is likely that there may be additional sources of CS_2 currently being under-estimated or not being accounted for, suggesting primarily that anthropogenic emissions are likely to be much larger than current estimates. In addition, the coarse resolution of STOCHEM model ($5°$ latitude $\times$ $5°$ longitude) makes it difficult to accurately model CS_2 in highly polluted areas which make up only a small fraction of the grid. The meteorological data incorporated in STOCHEM was from the year 1998 which was one of the strongest El Niño years in the past 50 years, this could lead to differences in the model data when compared with measured data from other years. Consideration of inter-annual variation give better representation of the model data which could improve the disagreement between model and measured data.

Figure 6 shows the vertical distributions of CS_2 over the North Atlantic, South tropical Atlantic, Western Pacific, Central/Eastern Pacific, Wallops Island-Virginia to Natal-Brazil, and Japan sea coast with the simulated data overlaid. The modeled CS_2 at different altitude levels for North Atlantic and South tropical Atlantic fit within one standard deviation of the measured mean except one outlier at 3.5 km. The STOCHEM-base case simulation underpredicted CS_2 by on average 1.5 ppt in North Atlantic and South tropical Atlantic and increasing the global ocean and soil emissions in the model, STOCHEM-OCSL reduces the underprediction by 47%. In the North Atlantic, the concentration at the surface is almost four times higher than that found in the South Atlantic because of the possible higher anthropogenic emissions of CS_2 in NH than that in SH. The global distribution of CS_2 (Figure 1) indicates that Europe and the east coast of the US have much higher concentrations compared with South America and Africa and thus through mixing and advection might have influenced CS_2 concentrations above the ocean [64]. In addition, the area of the South Atlantic that was sampled in this study was closer to the equator, thus higher OH concentrations yielding increased CS_2 removal and lower atmospheric concentrations.

In extremely polluted environments e.g., the Japan sea-coast (part of the NASA Transport and Chemical Evolution over the Pacific (TRACE-P) campaign to investigate outflow from polluted Asian regions and clean air from the Pacific Ocean), STOCHEM-base underpredicted the CS_2 concentrations in the Japan sea-coast with a mean bias of -64 ppt suggesting that the emissions of CS_2 integrated in the model are likely to be underestimated. The long-range transport of CS_2 from the source regions on the Asian continental outflow mixing with marine air over the Japan Sea can be responsible for the higher CS_2 over Japan sea coast [63]. The coarse model resolution ($5° \times 5°$) of

STOCHEM is responsible for model underprediction over the Japan sea-coast because it cannot represent typical Asian continental pollution with sufficient spatial accuracy. Increasing the global anthropogenic emissions of CS_2 in the STOCHEM-ANTH model reduces the model-measurement mean bias to -55 ppt. There are some other marine flight campaigns as part of TRACE-P e.g., Western Pacific and Central/Eastern Pacific, where the mean bias for STOCHEM-base is found to be -3.2 ppt. STOCHEM-OCSL and STOCHEM-ANTH simulations reduces the mean biases to 22% and 53%, respectively. In the study, a more comprehensive regional comparison with the literature was intended but there is a lack of up-to-date measurement data, more field and flight measurement data would be invaluable to validate our model accuracy.
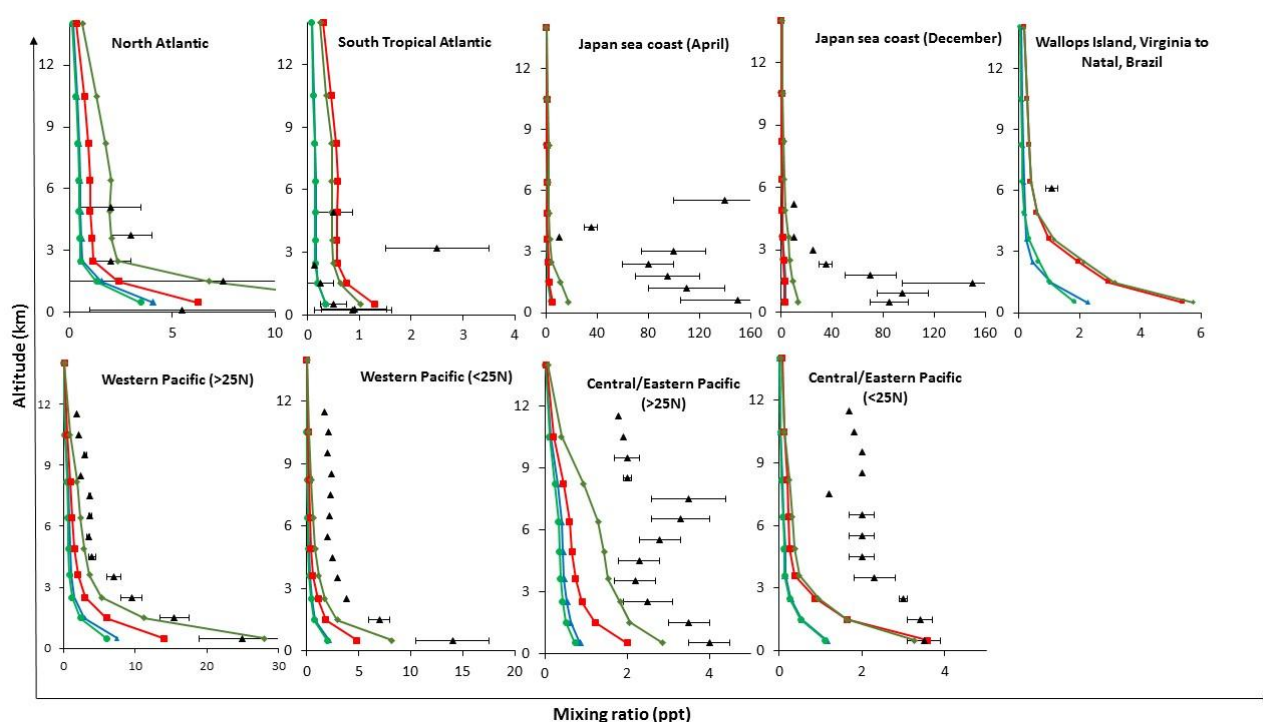
Figure 6. Vertical profiles for measured and modeled CS₂. Blue, green, red, and bottle green lines represent mean calculated values of CS₂ produced by the STOCHEM-base, STOCHEM-DEPO, STOCHEM-OCSL, and STOCHEM-ANTH, respectively. Black triangles represent the measurement CS₂ data and the black error bars represent measurement variability.

4. Conclusion

The global analysis for CS_2 was performed using a 3-D chemistry and transport model, STOCHEM-CRI which was concordant with several literature sources suggesting that the model results show a tendency towards underestimation. A suit of simulation results give the global burden and lifetime of CS_2 as 6.1 to 19.2 Tg and 2.8–3.4 days, respectively. The global surface distribution of CS_2 displayed the expected characteristics; with highest concentrations over areas of industrial activities. Comparing the global surface and vertical distribution of CS_2 simulated by the STOCHEM-CRI with other model studies suggested that the trends are found to be in good

agreement with the concentrations simulated by IMAGES and ECHAM3. The oxidation of CS_2 produces a large amount (0.5–1.9 Tg/yr) of OCS which can reduce the imbalance between the sources and the sinks of OCS. Increasing oceanic emissions in the model reduces the model-measurement disagreement significantly for the marine campaigns. The major underprediction by the model in polluted areas is likely due to the level of anthropogenic emissions being much greater than previously thought but also due to the coarse resolution of STOCHEM. Currently many of the campaigns have looked at very similar areas, for example the Global Tropospheric Experiment/Chemical Instrumentation Test and Evaluation (GTE/CITE 3) and Global Atmospheric Measurements Experiment of Tropospheric Aerosols and Gases (GAMETAG) expeditions have carried out extensive sampling around the East coast of USA, the Atlantic Ocean and down to South America. The TRACE-P study looked in detail at China, South East Asia, Korea and Japan, yet there has been very little sampling from Europe, the Middle East and the SH in general. Such experimental data will be the key to validate our model results.

Acknowledgements

Conflict of interest

We declare that there is no conflict of interest in this paper.

References

1. Wine PH, Chameides WL, Ravishankara AR (1981) Potential role of CS2 photooxidation in tropospheric sulfur chemistry. *Geophys Res Lett* 8: 543-546.
2. Andreae MO (1990) Ocean-atmosphere interactions in the global biogeochemical sulfur cycle. *Mar Chem* 30: 1-29.
3. Khalil MAK, Rasmussen RA (1984) Global sources, lifetimes and mass balances of carbonyl sulphide (OCS) and carbon disulfide (CS_2) in the Earth's atmosphere. *Atmos Environ* 18: 1805-1813.
4. Leck C, Rodhe H (1991) Emissions of marine biogenic sulfur to the atmosphere of northern Europe. *J Atmos Chem* 12: 63-86.
5. Kim K-H, Andreae MO (1992) Carbon disulfide in the estuarine, coastal, and oceanic environments. *Marine Chem* 40: 179-197.
6. Xie H, Moore RM, Miller WL (1998) Photochemical production of carbon disulphide in seawater. *J Geophys Res* 103: 5635-5644.
7. Xie H, Moore RM, Miller WL (1999) Carbon disulfide in the North Atlantic and Pacific oceans. *J Geophys Res* 104: 5393-5402.
8. Kettle AJ, Rhee TS, von Hobe M, et al. (2001) Assessing the flux of different volatile sulfur gases from the ocean to the atmosphere. *J Geophys Res* 106: 12193-12209.
9. Chin M, Davis DD (1993) Global sources and sinks of OCS and CS_2 and their distributions. *Global Biogeochem. Cycles* 7: 321-337.

10. Watts SF (2000) The mass budgets of carbonyl sufide, dimethyl sulphide, carbon disulfide and hydrogen sulphide. *Atmos Environ* 34: 761-779.

11. Blake NJ, Streets DG, Woo JH, et al. (2004) Carbonyl sulphide and carbon disulfide: large-scale distributions over the western Pacific and emissions from Asia during TRACE-P. *J Geophys Res* 109: D15.

12. Ren YL (1999) Is carbonyl sulfide a precursor for carbon disulfide in vegetation and soil? Interconversion of carbonyl sulfide and carbon disulfide in fresh grain tissues in vitro. *J Agric Food Chem* 47: 2141-2144.

13. Steinbacher M, Bingemer HG, Schmidt U (2004) Measurements of the exchange of carbonyl sulfide (OCS) and carbon disulfide (CS_2) between soil and atmosphere in a spruce forest in central Germany. *Atmos Environ* 38: 6043-6052.

14. Stickel RE, Chin M, Daykin EP, et al. (1993). Mechanistic studies of the OH-initiated oxidation of CS_2 in the presence of O_2. *J Phys Chem* 97: 13653-13661.

15. Seinfeld JH, Pandis SN (2006) Atmospheric Chemistry and Physics: From Air Pollution to Climate Change, 2 Eds., John Wiley and Sons, Inc., New Jersey: 1-1203.

16. Crutzen PJ (1976) The possible importance of CSO for the sulfate layer of the stratosphere. *Geophys Res Lett* 3: 73-76.

17. Hofmann DJ (1990) Increase in the stratospheric background sulfuric acid aerosol mass in the past 10 years. *Science* 248: 996-1000.

18. Taubman SJ, Kasting JF (1995). Carbonyl sufide: No remedy for global warming. *Geophys Res Lett* 22: 803-805.

19. Chin M, Davis DD (1995) A reanalysis of carbonyl sulphide as a source of stratospheric background sulfur aerosol. *J Geophys Res Atmos* 100: 8993-9005.

20. Bruhl C, Lelieveld J, Tost H, et al. (2015). Stratospheric sulfur and its implications for radiative forcing simulated by the chemistry climate model EMAC. *J Geophys Res-Atmos* 120: 2103-2118.

21. Xu X, Bingemer HG, Schmidt U (2002) The flux of carbonyl sulphide and carbon disulfide between the atmosphere and a spruce forest. *Atmos Chem Phys* 2: 171-181.

22. Taylor Jr GE, McLaughlin Jr SB, Shriner DS, et al. (1983). The flux sulfur-containing gases to vegetation. *Atmos Environ* 17: 789-796.

23. De Bruyn WL, Swartz E, Hu JH, et al. (1995) Henry's law solubilities and setchenow coefficients for biogenic reduced sulfur species obtained from gas-liquid uptake measurements. *J Geophys Res* 100: 7245-7251.

24. Berglen TF, Berntsen TK, Isaksen SA, et al. (2004) A global model of the coupled sulphur/oxidant chemistry in the troposphere: The sulphur cycle. *J Geophys Res* 109: D19310.

25. Kloster S, Feichter J, Maier-Reimer E, et al. (2006) DMS cycle in the marine ocean-atmosphere system- a global model study. *Biogeosciences* 3: 29-51.

26. Kettle AJ, Kuhn U, Von Hobe M, et al. (2002) Global budget of atmospheric carbonyl sulfide: Temporal and spatial variations of the dominant sources and sinks. *J Geophys Res* 107: D22.

27. Suntharalingam P, Kettle AJ, Monzka SM, et al. (2008) Global 3-D model analysis of the seasonal cycle of atmospheric carbonyl sulfide: Implications for terrestrial vegetation uptake. *Geophys Res Lett* 35: L19801.

28. Berry J, Wolf A, Campbell JE, et al. (2013) A coupled model of the global cycles of carbonyl sulfide and CO_2: A possible new window on the carbon cycle. *J Geophys Res-Biogeo* 118: 842-852.

29. Kuai L, Worden JR, Campbell JE, et al. (2015) Estimate of carbonyl sulfide tropical oceanic surface fluxes using Aura Tropospheric Emission Spectrometer observations. *J Geophys Res-Atmos* 120: 11012-11023.

30. Glatthor N, Höpfner M, Baker IT, et al. (2015) Tropical sources and sinks of carbonyl sulfide observed from space. *Geophys Res Lett* 42: 10082-10090.

31. Kremser S, Thomason LW, von Hobe M, et al. (2016) Stratospheric aerosol-Observations, processes, and impact on climate. *Rev Geophys* 54: 278-335.

32. Lennartz ST, Marandino CA, von Hobe M, et al. (2017) Direct oceanic emissions unlikely to account for the missing source of atmospheric carbonyl sulfide. *Atmos Chem Phys* 17: 385-402.

33. Pham M, Müller J-F, Brasseur GP, et al. (1995) A three-dimensional study of the tropospheric sulfur cycle. *J Geophys Res* 100: 26061-26092.

34. Weisenstein DK, Yue GK, Ko MKW, et al. (1997) A two-dimensional model of sulfur species and aerosols. *J Geophys Res* 102: 13019-13035.

35. Kjellström E (1998) A three-dimensional global model study of carbonyl sulphide in the troposphere and the lower stratosphere. *J Atmos Chem* 29: 151-177.

36. Stevenson DS, Collins WJ, Johnson CE, et al. (1998) Intercomparison and evaluation of atmospheric transport in a Lagrangian model (STOCHEM), and an Eulerian model (UM), using ^{222}Rn as a short-lived tracer. *Quat J Royal Meteorol Soc* 124: 2477-3492.

37. Stevenson DS, Dentener FJ, Schultz MG, et al. (2006) Multimodel ensemble simulations of present-day and near-future tropospheric ozone. *J Geophys Res* 111: D08301.

38. Collins WJ, Stevenson DS, Johnson CE, et al. (1997) Tropospheric ozone in a Global-Scale Three-Dimensional Lagrangian Model and its response to NO_x emission controls. *J Atmos Chem* 26: 223-274.

39. Utembe SR, Cooke MC, Archibald AT, et al. (2010) Using a reduced Common Representative Intermediates (CRI v2-R5) mechanism to simulate tropospheric ozone in a 3-D Lagrangian chemistry transport model. *Atmos Environ* 13: 1609-1622.

40. Derwent RG, Collins WJ, Jenkin ME, et al. (2003) The global distribution of secondary particulate matter in a 3-D Lagrangian chemistry transport model. *J Atmos Chem* 44: 57-95.

41. Stevenson DS, Johnson CE, Highwood EJ, et al. (2003) Atmospheric impact of the 1783–1784 Laki eruption: Part I chemistry modelling. *Atmos Chem Phys* 3: 487-507.

42. Derwent RG, Stevenson DS, Doherty RM, et al. (2008) How is surface ozone in Europe linked to Asian and North American NO_x emissions? *Atmos Environ* 42: 7412-7422.

43. Jenkin ME, Watson LA, Utembe SR, et al. (2008) A Common Representative Intermediate (CRI) mechanism for VOC degradation. Part-1: gas phase mechanism development. *Atmos Environ* 42: 7185-7195.

44. Watson LA, Shallcross DE, Utembe SR, et al. (2008) A Common Representative Intermediate (CRI) mechanism for VOC degradation. Part 2: gas phase mechanism reduction. *Atmos Environ* 42: 7196-7204.

45. Utembe SR, Watson LA, Shallcross DE, et al. (2009) A Common Representative Intermediates (CRI) mechanism for VOC degradation. Part 3: Development of a secondary organic aerosol module. *Atmos Environ* 43: 1982-1990.

46. Utembe SR, Cooke MC, Archibald AT, et al. (2011) Simulating secondary organic aerosol in a 3-D Lagrangian chemistry transport model using the reduced Common Representative Intermediates mechansim (CRI v2-R5). *Atmos Environ* 45: 1604-1614.

47. Collins WJ, Stevenson DS, Johnson CE, et al. (2000) The European regional ozone distribution and its links with the global scale for the years 1992 and 2015. *Atmos Environ* 34: 255-267.

48. Olivier JG, Bouwman AF, Berdowski JJ, et al. (1996) Description of EDGAR Version 2.0: A set of global emission inventories of greenhouse gases and ozone-depleting substances for all anthropogenic and most natural sources on a per country basis and on 1 degree × 1 degree grid. Technical report, Netherlands Environmental Assessment Agency.

49. Olivier JGJ, Berdowski JJM (2001) Global emissions sources and sinks. Berdowski JJM, Guicherit R, Heij BJ (Eds.). *The Climate System*, Swets and Zeitlinger Publishers, Lisse, Netherlands.

50. Granier C, Lamarque JF, Mieville A, et al. (2005) POET, a database of surface emissions of ozone precursors. Available from: http://accent.aero.jussieu.fr/database_table_inventories.php.

51. Atkinson R, Baulch DL, Cox RA, et al. (2004) Evaluated kinetic and photochemical data for atmospheric chemistry: Volume I-gas phase reactions of O_x, HO_x, NO_x and SO_x species. *Atmos Chem Phys* 4: 1461-1738.

52. Khan MAH, Cooke MC, Utembe SR, et al. (2015) A study of global atmospheric budget and distribution of acetone using global atmospheric model STOCHEM-CRI. *Atmos Environ* 112: 269-277.

53. Sander SP, Friedl RR, Golden DM, et al. (2006) Chemical kinetics and photochemical data for use in atmospheric studies. Evaluation number 15, *JPL publication* 06-2, Jet Propulsion Laboratory, Pasadena, CA.

54. Lee CL, Brimblecombe P (2016) Anthropogenic contributions to global carbonyl sulfide, carbon disulfide and organosulfides fluxes. *Earth-Sci Rev* 160: 1-18.

55. Majozi T, Veldhuizen P (2015) The chemicals industry in South Africa. American Inst. Chem. Eng (AlChE) July: 46-51. Available from:
https://www.aiche.org/sites/default/files/cep/20150746.pdf

56. Kim KH, Swan H, Shon ZH, et al. (2004) Monitoring of reduced sulfur compounds in the atmosphere of Gosan, Jeju Island during the Spring of 2001. *Chemosphere* 54: 515-526.

57. Guo H, Simpson IJ, Ding AJ, et al. (2010) Carbonyl sulphide, dimethyl sulphide and carbon disulfide in the Pearl River Delta of southern China: Impact of anthropogenic and biogenic sources. *Atmos Environ* 44: 3805-3813.

58. Pal R, Kim KH, Jeon EC, et al. (2009) Reduced sulfur compounds in ambient air surrounding an industrial region in Korea. *Environ Monit Assess* 148: 109-125.

59. Yujing M, Hai W, Zhang X, et al. (2002) Impact of anthropogenic sources on carbonyl sulphide in Beijing City. *J Geophys Res* 107: D24.

60. Maroulis PJ, Bandy AR (1980) Measurements of atmospheric concentrations of CS_2 in the eastern United States. *Geophys Res Letts* 7: 681-684.

61. Jones BMR, Cox RA, Penkett SA (1983) Atmospheric chemistry of carbon disulphide. *J Atmos Chem* 1: 65-86.

62. Thornton DC, Bandy AR (1993). Sulfur dioxide and dimethyl sulfide in the central pacific troposphere. *J Atmos Chem* 17: 1-13.

63. Inomata Y, Hayashi M, Osada K, et al. (2006) Spatial distributions of volatile sulfur compounds in surface seawater and overlying atmosphere in the northwestern Pacific Ocean, eastern Indian Ocean, and Southern Ocean. *Global Biogeochem Cycles* 20: GB2022.

64. Cooper DJ, Saltzman ES (1993) Measurements of atmospheric dimethylsulphide, hydrogen

sulphide, and carbon disulfide during GTE/CITE 3. *J Geophys Res* 98: 23397-23409.

65. Inomata Y, Iwasaka Y, Osada K, et al. (2006) Vertical distributions of particles and sulfur gases (volatile sulfur compounds and SO_2) over East Asia: comparison with two aircraft-borne measurements under the Asian continental outflow in spring and winter. *Atmos Environ* 40: 430-444.

66. Bandy AR, Thornton DC, Johnson JE (1993) Carbon disulfide measurements in the atmosphere of the western north Atlantic and the northwestern south Atlantic oceans. *J Geophys Res-Atmos* 98: 23449-23457.